Received: 3 May 2016 | Accepted: 20 June 2016

DOI: 10.1111/cpr.12276

ORIGINAL ARTICLE

WILEY Cell Proliferation

Nanofibrous polycaprolactone scaffolds with adhered platelets stimulate proliferation of skin cells

K. Vocetkova[1,2,3,4] | M. Buzgo[1,2,3] | V. Sovkova[1,2] | D. Bezdekova[1,2] | P. Kneppo[4] | E. Amler[1,2,3]

[1]Department of Biophysics, 2nd Faculty of Medicine, Charles University in Prague, 150 06, Prague 5, Czech Republic

[2]Laboratory of Tissue Engineering, Institute of Experimental Medicine, Czech Academy of Sciences, 142 20, Prague 4, Czech Republic

[3]University Center for Energy Efficient Buildings, Czech Technical University in Prague, 273 43, Bustehrad, Czech Republic

[4]Faculty of Biomedical Engineering, Czech Technical University in Prague, 272 01, Kladno 2, Czech Republic

Correspondence
Karolina Vocetkova, Institute of Experimental Medicine, Czech Academy of Sciences, 1083 Videnska, Prague 142 20, Czech Republic.
Email: karolina_vocetkova@labdemo.cz

Abstract

Objectives: Faulty wound healing is a global healthcare problem. Chronic wounds are generally characterized by a reduction in availability of growth factors. New strategies are being developed to deliver growth factors more effectively.

Methods: In this study, we introduced electrospun scaffolds composed of polycaprolactone (PCL) nanofibers functionalized with adhered platelets, as a source of numerous growth factors. Three concentrations of platelets were immobilized to nanofibrous scaffolds by simple adhesion, and their influence on adhesion, proliferation and metabolic activity of seeded cells (murine fibroblasts, keratinocytes and melanocytes) was investigated.

Results: The data obtained indicated that presence of platelets significantly promoted cell spreading, proliferation and metabolic activity in all the skin-associated cell types. There were no significant differences among tested concentrations of platelets, thus even the lowest concentration sufficiently promoted proliferation of the seeded cells.

Conclusions: Such complex stimulation is needed for improved healing of chronic wounds. However, the nanofibrous system can be used not only as a skin cover, but also in broader applications in regenerative medicine.

1 | INTRODUCTION

Wound healing is a complex biological process mediated by the interaction of signal molecules and mesenchymal cells.[1] When the integrity of the epidermal barrier is disrupted, a blood clotting cascade is activated and platelets release numerous growth factors (GFs), such as epidermal growth factor (EGF), platelet-derived growth factor (PDGF) and transforming growth factor β (TGF-β).[2] The released GFs attract immune cells to remove contaminating bacteria and damaged tissue and stimulate fibroblasts' proliferation and synthesis of new extracellular matrix (ECM).[3] Within hours after the injury, re-epithelialization starts via the EGF stimulation of keratinocyte migration and proliferation. Once the wound is closed, keratinocytes undergo stratification and differentiation in order to restore the epidermal barrier. Disruption of the fine balance may result in a poorly healing wound.

Faulty wound healing is becoming a global healthcare problem.[4] According to Mustoe[5] the majority of chronic wounds can be classified into three categories—venous, diabetic and pressure ulcers. In the United States 1% of the population and up to 3.5% of people over 65 years of age suffer from venous ulcers.[6] The International Diabetic Federation in its 2014 report stated there are 387 million people living with diabetes worldwide, approximately 15% of them develop at least one diabetic ulcer. Effective wound dressings are thus needed.[4]

Wound dressings protect the wound and facilitate different aspects of healing.[4] Generally, they should provide a suitable microenvironment at the wound/dressing interface. They should absorb excess exudate, provide mechanical and bacterial protection and allow exchange of gases and fluids.[7] These requirements could be met by electrospun nanofibrous mats. Electrospinning is a unique technique that uses a strong electric field to generate polymeric nanofibers. Such fibers are of a nanoscale diameter and thus mimic the microarchitecture of the extracellular matrix. They exhibit high porosity, with the interconnected pores facilitating the exchange of nutrients and gases, moisturization of the wound and drainage of the excess fluid. Moreover, their

high surface to volume ratio favors the adsorption of bioactive compounds.[8] By incorporating bioactive compounds (e.g. growth factors) into the scaffold, one can mimic the function of ECM as well.[9]

Chronic wounds generally exhibit a decrease in the availability of growth factors (GFs).[1] GFs delivered exogenously are usually not very effective, since they tend to diffuse away from the wound and are enzymatically deactivated. Conventional ways of delivery (e.g. bolus administration) are thus less likely to obtain promising results. Currently, new strategies are being employed to deliver high concentrations of multiple endogenous GFs to the site of interest.[10]

Platelets are a natural source of growth factors. Their α-granules contain a large number of GFs, for instance platelet derived growth factor, transforming growth factor beta or epidermal growth factor. Platelets are typically used in hematological applications, however platelet-rich plasma (PRP) is gaining popularity in orthopedic and craniofacial surgery.[11] It is a simple and cost-effective way of delivering endogenous GFs.[12] To improve the bioavailability of the GFs, delivery systems serving as depots for the GFs are being developed.[10]

The aim of this study was to develop a drug delivery system that could serve as a wound dressing. Polycaprolactone (PCL) nanofibers were chosen as a scaffold. The scaffold was functionalized with three concentrations of immobilized platelets (maximum concentration and 2-fold and 4-fold dilution). Its efficacy was tested in vitro using keratinocytes, fibroblasts and melanocytes.

2 | MATERIALS AND METHODS

2.1 | Scaffold fabrication

PCL scaffolds were fabricated using the Nanospider™ technology (Elmarco Liberec, Czech Republic). Electrospinning is a fiber forming technology based on drawing a submicron fiber from solution or melt. The apparatus consists of a spinning electrode delivering the polymer and a collection electrode for depositing the prepared fibers. The electrodes are connected to a high-voltage power supply (0–140 kV) and upon action of the electric field, electrostatic forces emerge on the surface of the polymer solution. When electrostatic forces overcome the surface tension, fiber jets emit polymer droplets. The droplets are axially stretched and with an increase of the droplet surface, the solvent evaporates and solid fibers are deposited on the surface of the collector. To perform electrospinning, a 24% (w/v) solution of PCL (MW 40 000 Wako Chemicals GmbH, Neuss, Germany) dissolved in a mixture of chloroform and ethanol at ratio 9:1 was used. The solution was electrospun using a needleless wire electrode with deposits placed on a non-woven supporting textile (Spunbond, Pegas Textiles). The conditions during the electrospinning were maintained at 23 ± 2°C and 60 ± 15% relative humidity (RH).

2.2 | Scaffold characterization

In order to visualize the architecture of the scaffolds, the samples were analyzed using scanning electron microscopy. Samples were rinsed with phosphate buffer saline (PBS; 137 mmol L^{-1} NaCl, 2.7 mmol L^{-1} KCl, 10 mmol L^{-1} Na_2HPO_4, 1.8 mmol L^{-1} KH_2PO_4) and fixed with 2.5% glutaraldehyde for 4 hours at 4°C. Subsequently, the samples were washed with PBS, dehydrated with ethanol changes and treated with HMDS. Afterwards, the samples were sputter coated with gold using Quorum Q150RS. A Vega3 SBU (Tescan, Brno, Czech Republic) microscope was used for observation. The mean diameter of the fibers and pore size was determined from the acquired images in ImageJ software from at least 200 independent measurements.

2.3 | Composite scaffold preparation

PCL samples (diameter 6 mm) were punched out of the electrospun matt. The samples were sterilized using 70% ethanol and rinsed with PBS. Human leukocyte-depleted platelet concentrate derived from buffy-coat (in additive solution) was obtained from Blood Transfusion Service (Šumperk, Czech Republic). Three concentrations C1 (1.03×10^{12} platelets/L, maximum concentration), C2 (5.15×10^{11} platelets/L, half the maximum concentration) and C3 (2.575×10^{11} platelet/L, quarter the maximum concentration) were prepared and 50 μL of the solutions were added to the sterile nanofibrous samples in a 96-well plate. Additive solution was used to dilute the platelet concentrate. Samples were incubated for 2 hours at a temperature of 22°C. Afterwards, the samples were washed with PBS and placed into new wells.

2.4 | Cell culture conditions & Cell seeding

A Murine melan-a cell line (melanocytes) and murine XB2 cell line (keratinocytes) were purchased from Welcome Trust Functional Genomics Cell Bank at St. George's, University of London. A Murine 3T3-A31 cell line was purchased from Sigma-Aldrich, Munich, Germany (Germany). All cell lines were cultured in a humidified incubator (37°C, 10% CO_2 and 80–90% RH). Dulbecco's modified Eagle's medium supplemented with 10% fetal bovine serum (FBS) and penicillin/streptomycin (100 IU/mL, 100 μg/mL) was used for culture of fibroblasts and keratinocytes; RPMI-1640 medium with 10% FBS, penicillin/streptomycin (100 IU/mL, 100 μg/mL), 2 mmol L^{-1} L-glutamine and 200 nmol L^{-1} TPA (12-O-tetradecanoylphorbol-13-acetate) was used for melanocytes. TPA is a tumor promoter needed for the proliferation of melanocytes, as they are generally cells of a very low proliferative potential. Without the addition of TPA, no net proliferation of the cells occurs.[13] However, its tumorigenic effect excludes it from clinical practice. The media were changed every 3–4 days. Subconfluent cells were washed with PBS containing 0.02% (w/v) ethylenediaminetetraacetic acid (EDTA) and treated with trypsin/EDTA solution. The detached cells were counted using a hemocytometer. The scaffolds were seeded with keratinocytes (7800 cells/cm^2), fibroblasts (7800 cells/cm^2) and melanocytes (12 500 cells/cm^2).

2.5 | Cell metabolic activity testing

The metabolic activity of cells was determined on day 1, 3, 7 and 14 using the MTS assay (CellTiter96® AQ_{ueous} One Solution Cell

Proliferation Assay; Promega, Madison, WI, USA). To each scaffold, 20 μL of MTS solution and 100 μL of fresh medium were added. After incubation (37°C, 10% CO_2, 80–90% RH) the absorbance of the media was detected at 490 nm with a microplate reader (Infinite® M200 PRO; Tecan, Männedorf, Switzerland). The background absorbance (690 nm) was subtracted from the measured data, as well as the absorbance of plain media. Platelets contain mitochondrial enzymes and thus metabolize the MTS substrate. To exclude misrepresentation of the cell metabolic activity due to the presence of platelets, an MTS assay of samples with platelets was performed. The detected absorbance was subtracted from the measured data.

2.6 | Cell proliferation testing

To determine the cell proliferation a fluorescence-based kit (Quant-iT™ PicoGreen® dsDNA Assay Kit; Invitrogen, Carlsbad, CA, USA) was used. The samples used for the MTS assay were transferred to 500 μL of cell lysis buffer (10 mmol L^{-1} Tris, 1 mmol L^{-1} EDTA, 0.2% v/v Triton X-100). To facilitate the cell lysis and DNA release, the samples underwent three freeze/thaw cycles. In between the cycles, the samples were vortexed. Fluorescence intensity was detected using a microplate reader (λ_{ex} = 485 nm, λ_{em} = 528 nm) and the DNA content was determined according to the λDNA calibration curve of the kit.

2.7 | Cell visualization

Confocal microscopy was used to visualize the cells. The cells seeded on scaffolds were fixed with methanol (−20°C), rinsed with PBS and stained. DiOC6 was used to visualize the cellular membranes (1 μg/mL in PBS, 30 minute) and propidium iodide (5 μl/mL, 10 minute) to visualize the cell nuclei. Between the incubations the samples were rinsed with PBS. A Zeiss LSM 510 DUO confocal microscope was used for imaging (λ_{ex} = 488 nm, λ_{em} = 501 nm for DiOC6; λ_{ex} = 536 nm, λ_{em} = 617 nm for propidium iodide). In case of melanocytes, confocal images were merged with images scanned in visible light to visualize the melanin present on the scaffolds.

2.8 | Melanin content

Melanin content on the scaffolds was determined according to Busca et al.[14] with minor alterations. Briefly, samples were transferred to 300 μL of 1 mol L^{-1} NaOH and incubated for 2 hours at 80°C. Afterwards, the samples were vortexed to facilitate solubilization of melanin and centrifuged (10 000 ***g***, 1 minute, MiniSpin®; Eppendorf, Hamburg, Germany) to sediment the PCL debris. Absorbance of the supernatant was detected at 405 nm using a microplate reader. The melanin content on the scaffolds was determined according to a calibration curve (synthetic melanin; Sigma-Aldrich).

2.9 | Release of EGF from the scaffold

To determine the release profiles of growth factors from the platelet-functionalized samples, EGF was chosen as a model molecule. EGF stimulates proliferation of keratinocytes and fibroblasts, thus accelerates reepithelialization and increases tensile strength of the wound.[2] On every day of the experiment, cell culture media were collected and frozen (−80°C). The concentration of EGF released from platelets and/or synthetized by the seeded cells was quantified by conducting the enzyme-linked immunosorbent assay (ELISA) in accordance with the manufacturer's instructions (DuoSet®; R&D Systems, Minneapolis, MN, USA).

2.10 | Statistical analysis

The data were statistically evaluated using SigmaStat 3.5 software. Statistical significance between a pair of groups with normal distribution was determined using ANOVA testing. The data are presented as mean values plus or minus the standard deviation. A value of $P<.05$ was considered statistically significant.

3 | RESULTS

3.1 | Scaffold characterization

The architecture of the prepared scaffolds was investigated using scanning electron microscopy (Fig. 1). The samples showed architecture typical for PCL nanofibers. The analysis showed nano-/microarchitecture with a minimum of non-fibrous defects. The mean diameter of the thin nanofibrous fraction was 241.6 ± 90.6 nm, the thicker fibers had a mean diameter of 748 ± 147.4 nm. In addition, a less abundant microfibrous fraction was detected with a mean diameter of 1486.8 ± 419.1 nm. The mean pore size was 10.28 ± 12.1 μm. On the platelet-functionalized samples, platelets were activated due to their contact with the nanotopography of the prepared nanofibrous layer and subsequently changed their morphology. Furthermore, a clear thick fibrin layer was observed on the platelet-functionalized PCL samples (Fig. 1a–c).

3.2 | Keratinocytes

To test the biocompatibility of the scaffolds, the metabolic activity of the seeded cells on platelet-functionalized scaffolds (C1 – maximum platelet concentration, C2 – half the maximum platelet concentration, C3 – quarter the maximum platelet concentration) was determined. Figure 2a shows the metabolic activity of keratinocytes. During the experiment there was no clear tendency in the acquired data. On day 14 the metabolic activity of keratinocytes was significantly higher on the C3 sample (quarter the maximum platelet concentration) in comparison to the PCL control ($P<.05$).

Proliferation of keratinocytes seeded on nanofibrous scaffolds is shown in Fig. 2b. Until day 14 there was no significant difference in keratinocyte proliferation between the samples. On day 14 all the samples containing platelets exhibited a significant increase in cell proliferation in comparison to PCL ($P<.05$). There were significant differences among the C-samples. On the C1 sample the amount of synthetized DNA was significantly larger in comparison to the C2 and

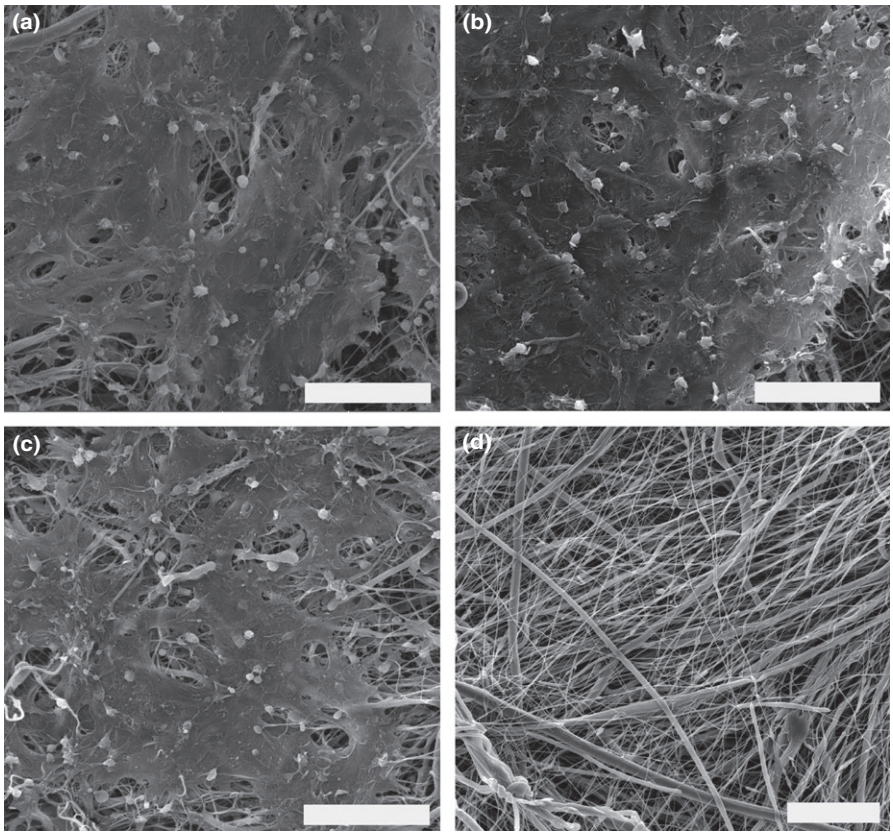

FIGURE 1 Scanning electron microscopy images of the nanofibrous scaffolds. (a) C1 scaffold (PCL scaffold functionalized with maximum platelet concentration, scale bar 20 μm, magnification 4000×). (b) C2 scaffold (PCL with half the maximum platelet concentration, scale 20 μm, magnification 4000×), (c) C3 scaffold (PCL with quarter the maximum platelet concentration, scale bar 20 μm, magnification 4000×). (d) PCL control scaffold (scale bar 20 μm, magnification 2940×)

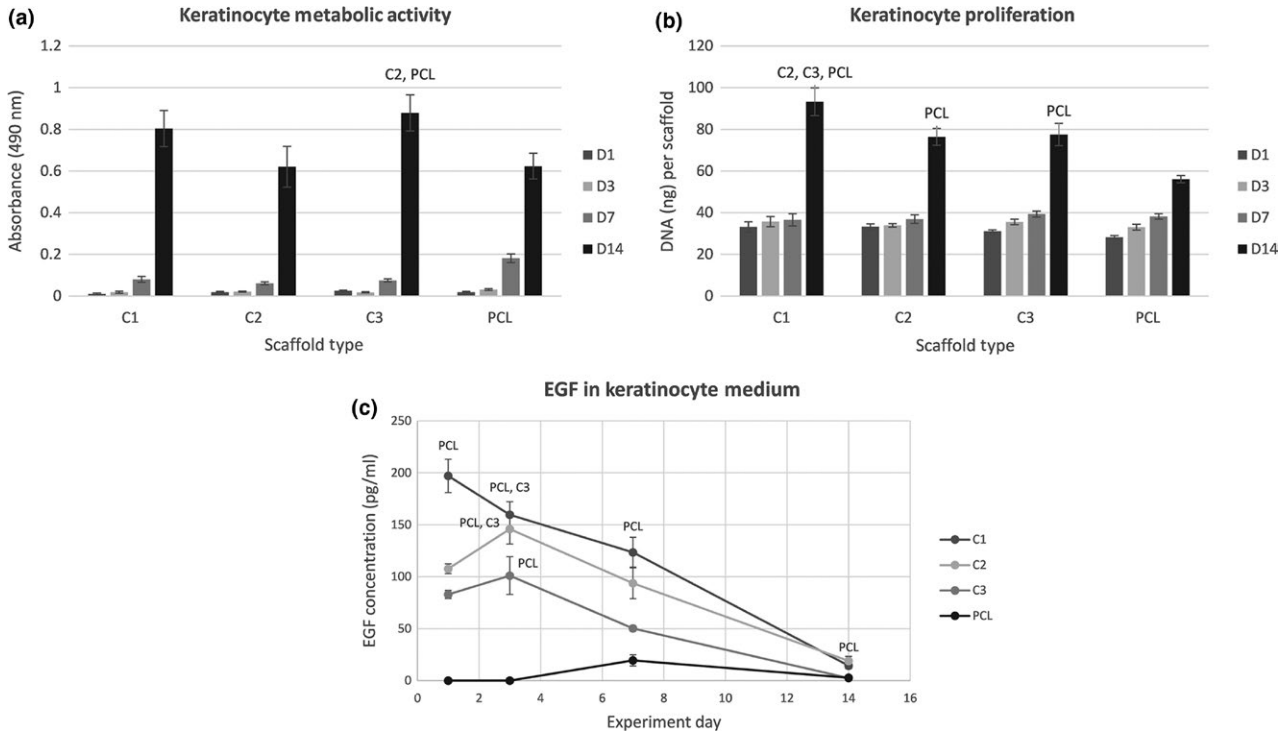

FIGURE 2 Keratinocyte metabolic activity, proliferation and detection of EGF levels. (a) Metabolic activity of keratinocytes measured by MTS assay (statistical analysis $P<.05$). (b) Proliferation of keratinocytes determined by PicoGreen® assay (statistical analysis $P<.05$). (c) Concentration of EGF in the keratinocyte culture medium determined by ELISA (statistical analysis $P<.05$)

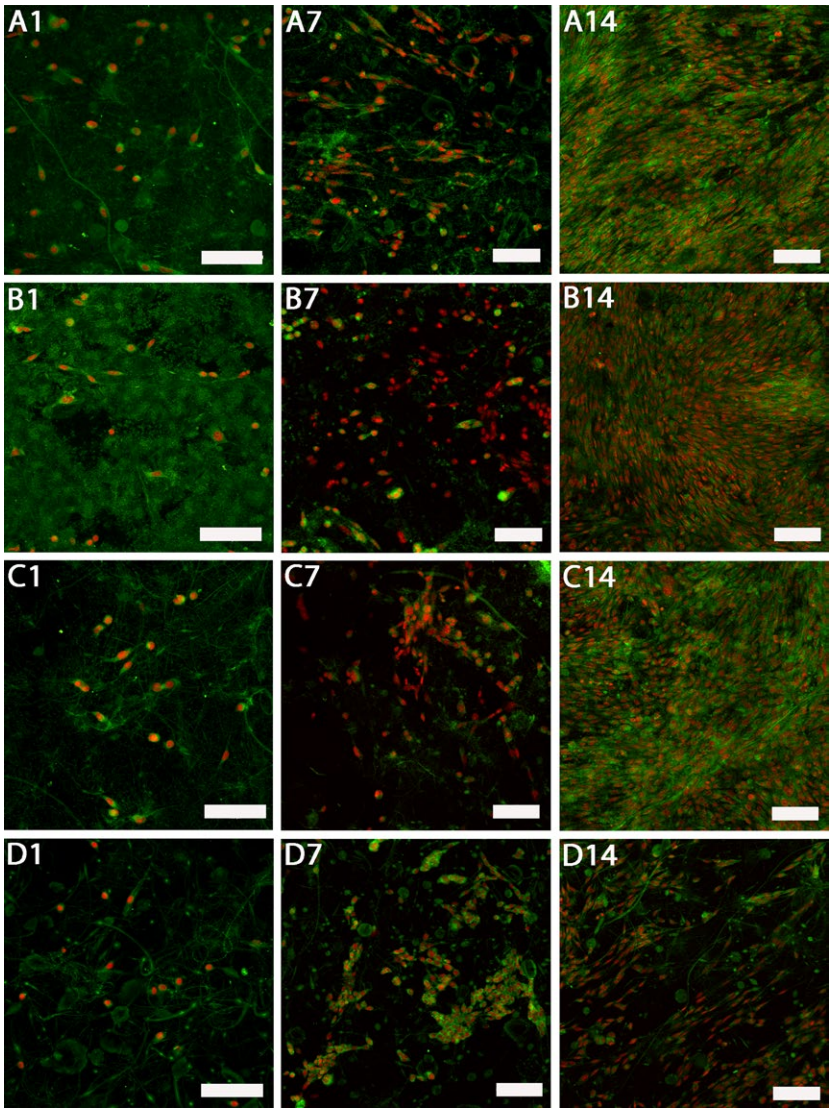

FIGURE 3 Confocal images of keratinocytes cultured on platelet-functionalized PCL and PCL control scaffolds. Cellular membranes were stained by DiOC-6 (green color), cell nuclei using propidium iodide (red color). A1 – Keratinocytes cultured on C1 scaffold on day 1, A7 – keratinocytes cultured on C1 scaffold on day 7, A14 – keratinocytes cultured on C1 scaffold on day 14, B1 – keratinocytes cultured on C2 scaffold on day 1, B7 – keratinocytes cultured on C2 scaffold on day 7, B14 – keratinocytes cultured on C2 scaffold on day 14, C1 – keratinocytes cultured on C3 scaffold on day 1, C7 – keratinocytes cultured on C3 scaffold on day 7, C14 – keratinocytes cultured on C3 scaffold on day 14, D1 – keratinocytes cultured on PCL scaffold on day 1, D7 – keratinocytes cultured on PCL scaffold on day 7, D14 – keratinocytes cultured on PCL scaffold on day 14. A1, B1, C1, D1 – scale bar 100 μm, magnification 200x, A7, A14, B7, B14, C7, C14, D7, D14 – scale bar 100 μm, magnification 150×

C3 samples ($P<.05$). Keratinocytes attached to the samples were visualized using laser scanning confocal microscopy on day 1, 7 and 14 (Fig. 3). On day 14 the keratinocyte monolayers were confluent on all the samples containing platelets. On the contrary, the number of cells on the PCL control sample did not increase so dramatically between day 7 and 14 of the experiment.

The concentration of released EGF was determined by ELISA in the media collected from the samples with seeded keratinocytes (see Fig. 2c). At the beginning of the experiment, the highest concentration of EGF was in sample C1. The concentration of EGF was accordingly lower at samples C2 and C3. During the experiment, EGF levels in the cell culture medium were gradually decreasing. On the PCL control samples, synthesis of EGF by the seeded keratinocytes was observed by day 7 of the experiment.

3.3 | Fibroblasts

The metabolic activity of fibroblasts seeded on platelet-functionalized samples (C1 – maximum platelet concentration, C2 – half the maximum platelet concentration, C3 – quarter the maximum platelet concentration) is shown in Fig. 4a. Through the whole experiment the metabolic activity of fibroblasts on the C3 scaffold was significantly higher in comparison to the PCL scaffold ($P<.05$). In addition to that, on day 1, 3 and 7 the metabolic activity of fibroblasts on the C3 scaffold was significantly higher than the metabolic activity of cells on scaffolds C1 and C2 ($P<.05$). From day 7 the metabolic activity of cells on the C-samples was significantly improved in comparison to PCL control ($P<.05$). On day 14 there were no statistically significant differences in the cell metabolic activity on the scaffolds functionalized with platelets.

Proliferation of fibroblasts (Fig. 4b) was determined on day 1, 3, 7 and 14. There was no significant difference in the amount of the synthetized DNA between the samples with platelets and the PCL control until day 7 of the experiment. On day 7 and 14 there was a significantly larger amount of DNA on the scaffolds with platelets in comparison to the control sample ($P<.05$). There were no significant differences among the C-samples.

Fibroblasts visualization can be seen in Fig. 5. On day 14 the fibroblast monolayers on samples with immobilized platelets were almost

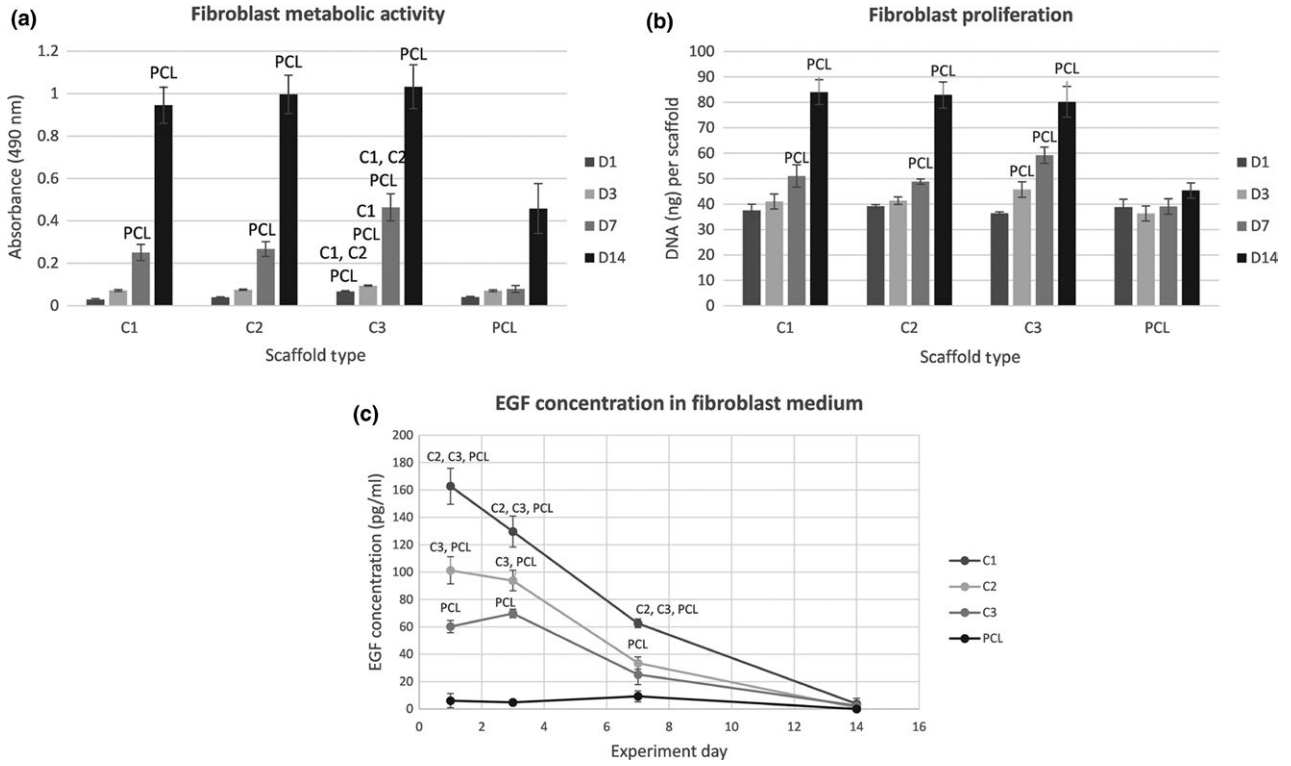

FIGURE 4 Fibroblast metabolic activity, proliferation and detection of EGF level. (a) Metabolic activity of fibroblasts measured by MTS assay (statistical analysis $P<.05$). (b) Proliferation of fibroblasts determined by PicoGreen® assay (statistical analysis $P<.05$). (c) Concentration of EGF in the fibroblast culture medium determined by ELISA (statistical analysis $P<.05$)

confluent, contrary to the control sample. There were no significant differences among the samples with platelets.

The levels of EGF released to the fibroblast culture media were determined on the days of the experiment using the ELISA, see Fig. 4c. There were significant differences in the EGF concentration among the C-samples ($P<.05$), corresponding to the seeding platelet concentration. Through the experiment, the concentrations of EGF in the fibroblast media were gradually decreasing. On the PCL control sample, synthesis of EGF by fibroblasts was observed. However, the levels of EGF detected in the control samples were significantly lower than the levels of EGF delivered by the adhered platelets in the platelet-functionalized samples.

3.4 | Melanocytes

The metabolic activity of melanocytes seeded on the platelet-functionalized samples (C1 – maximum platelet concentration, C2 – half the maximum platelet concentration and C3 – quarter the maximum platelet concentration) can be seen in Fig. 6a. During the whole experiment the metabolic activity of melanocytes on samples with platelets was significantly higher in comparison to plain PCL ($P<.001$). There were no statistically significant differences among the C-samples.

The amount of synthetized DNA by melanocytes was determined as described above (see Fig. 6b). The data show the proliferation of melanocytes was increasing through the whole experiment. Platelets significantly promoted melanocyte proliferation on all the platelet-functionalized scaffolds from day 7 in comparison to PCL control ($P<.05$). There were no significant differences among the C-samples in melanocyte proliferation.

The amount of melanin synthetized by melanocytes on the nanofibrous scaffolds (Fig. 6d) was increasing throughout the whole experiment. On day 7, there was a significantly larger amount of melanin on scaffold C1 in comparison to plain PCL nanofibers ($P<.05$). On day 14, the amount of synthetized melanin was significantly larger on scaffolds C2 and C3, in comparison to PCL control ($P<.05$).

Figure 7 shows melanocyte proliferation during the experiment. The number of melanocytes on the scaffolds with platelets increased between day 1 and day 7. On day 7, the monolayers of the cells were almost confluent and no significant difference was observed on day 14. The PCL control showed the same trend, but the overall number of cells was significantly lower than on the platelet-functionalized C-samples and the cell monolayers were not confluent even by day 14 of the experiment. In addition to that, synthetized melanin was present on the scaffolds. The melanin is depicted by the color black in confocal images merged with images in visible light.

4 | DISCUSSION

The wound healing cascade is governed by the interplay of multiple stimuli.[15] Growth factors are among the most important regulatory

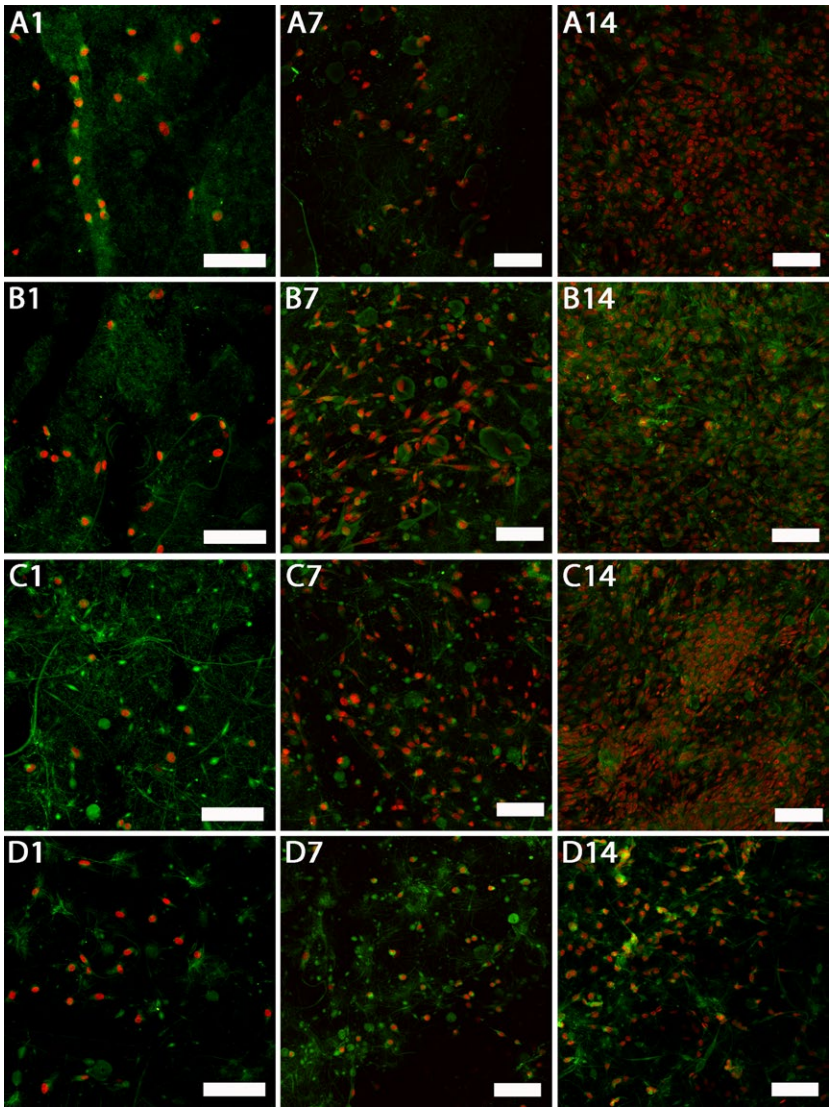

FIGURE 5 Confocal images of fibroblasts cultured on platelet-functionalized PCL and PCL control scaffolds. Cellular membranes were stained by DiOC-6 (green color), cell nuclei using propidium iodide (red color). A1 – Fibroblasts cultured on C1 scaffold on day 1, A7 – fibroblasts cultured on C1 scaffold on day 7, A14 – fibroblasts cultured on C1 scaffold on day 14, B1 – fibroblasts cultured on C2 scaffold on day 1, B7 – fibroblasts cultured on C2 scaffold on day 7, B14 – fibroblasts cultured on C2 scaffold on day 14, C1 – fibroblasts cultured on C3 scaffold on day 1, C7 – fibroblasts cultured on C3 scaffold on day 7, C14 – fibroblasts cultured on C3 scaffold on day 14, D1 – fibroblasts cultured on PCL scaffold on day 1, D7 – fibroblasts cultured on PCL scaffold on day 7, D14 – fibroblasts cultured on PCL scaffold on day 14. A1, B1, C1, D1 – scale bar 100 μm, magnification 200x, A7, A14, B7, B14, C7, C14, D7, D14 – scale bar 100 μm, magnification 150×

agents. Even small deviations in the coordination of the cellular processes and appropriate GF levels may result in the inability of the wound to close.[2]

The aim of this study was to develop a nanofibrous wound dressing enriched with growth factors. Platelets were chosen as a source of multiple growth factors efficient in wound healing (EGF, PDGF, TGF-β).[16] PDGF acts as a strong fibroblast mitogen and plays an important role in all stages of wound healing, including angiogenesis and reepithelization. TGF-β promotes fibroblast proliferation and extracellular matrix production. EGF not only stimulates fibroblast proliferation, but keratinocyte proliferation as well.[17] Further growth factors, contained in platelets, such as bFGF and HGF have been described to be important for the proper growth of melanocytes.[18] Three different platelet concentrations were tested, to investigate the influence of the mixture of growth factors on the skin cell lines.

The platelet-nanofiber composite was prepared by adhesion of platelets to PCL nanofibers. The nanofibers exhibited architecture typical for PCL. The samples contained a mixture of nano- and microfibers. Similar architecture was observed by Plencner et al.[19] and Knotek et al.[20] The nano/micro structure combines higher pore size between microfibers with the high adhesion capacity of the nanofibrous part.[21] Importantly, we have demonstrated that platelets were efficiently absorbed on the surface of nanofibers.

Scanning electron microscopy showed that the platelets were activated upon adhesion to the scaffold surface and a thick fibrin network was formed. Such findings are in agreement with Wan and Xu.[22] They demonstrated platelets undergo activation upon adhesion to nanofibers thanks to their specific surface topography. The natural character of fibrin has been widely used in various tissue engineering applications. The fibrin network formed promotes cellular adhesion via integrin and non-integrin receptors.[23] Such biomimetic motives are crucial for the enhancement of cellular adhesion and proliferation on the rather hydrophobic surface of PCL scaffolds. Additionally, other natural polymers are being used to enhance the scaffold biocompatibility and cellular interactions, such as collagen[24] or chitosan.[25] A similar system composed of platelets adhered to PCL nanofibrous mesh was tested by Jakubova et al.[26] and Plencner et al.[19] Jakubova et al.[26] tested the influence of platelets adhered to PCL on chondrocyte proliferation,

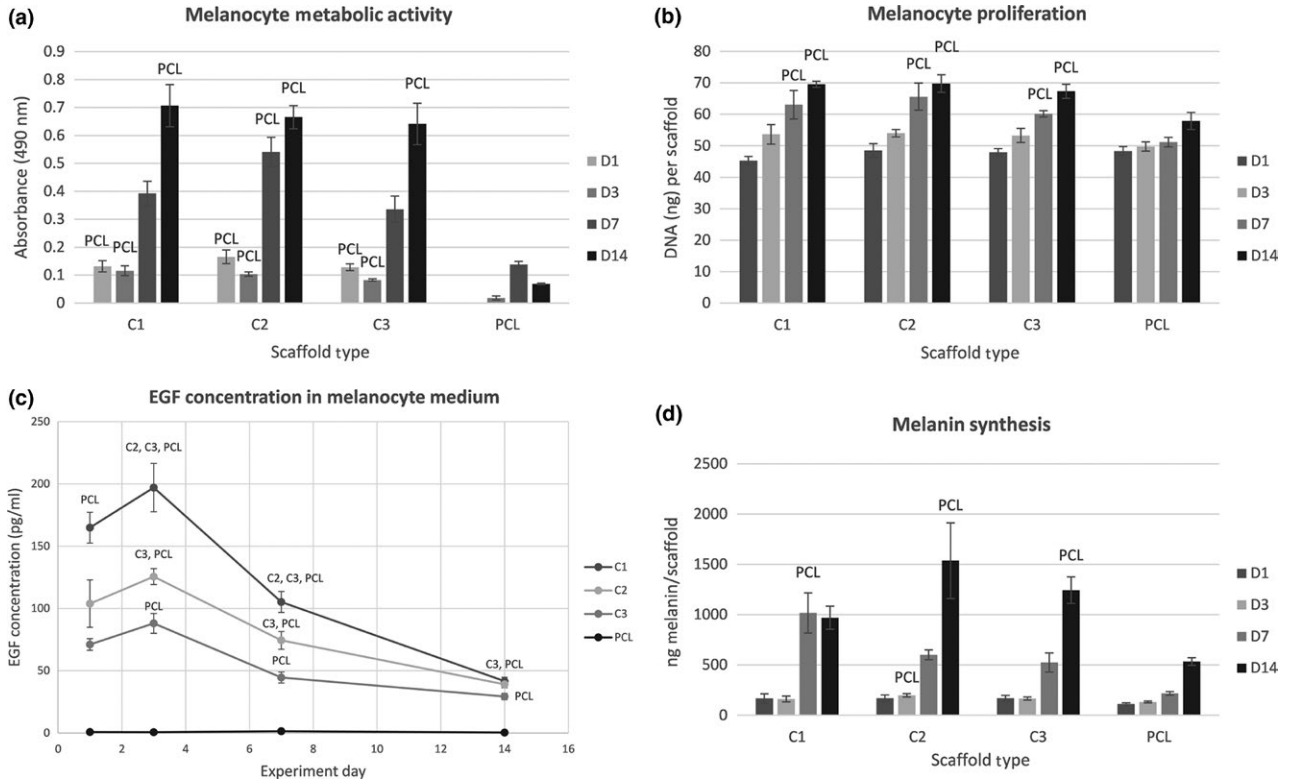

FIGURE 6 Melanocyte metabolic activity, proliferation, detection of EGF levels and synthesis of melanin. (a) Metabolic activity of melanocytes measured by MTS assay (statistical analysis $P<.05$). (b) Proliferation of melanocytes determined by PicoGreen® assay (statistical analysis $P<.05$). (c) Concentration of EGF in the melanocyte culture medium determined by ELISA (statistical analysis $P<.05$). (d) Melanin synthesis on the scaffolds determined by NaOH assay (statistical analysis $P<.05$)

Plencner et al. [19] utilized such a system in ventral hernia regeneration. Both studies showed a significant improvement of cell metabolic activity and proliferation due to the bioactive substances released from platelets.

The prepared system was utilized to culture keratinocytes. The results indicate that the released growth factors stimulated metabolic activity and proliferation on the platelet-functionalized samples in comparison to the plain PCL scaffold. However, the stimulatory effect seemed to be independent of the initial platelet concentration. Our confocal microscopy studies of the morphology of the keratinocytes showed confluent layers of distinctively stratified and differentiated cells on all the platelets containing samples. It has been reported that sufficiently high concentrations of EGF result in keratinocyte proliferation and differentiation, promoting wound healing in diabetic mice.[27]

Furthermore, a composite system was used to culture fibroblasts. Stimulation of fibroblast proliferation and ECM production in the presence of platelets was described by Liu et al.[28] Our study showed that the adhered platelets stimulated cell metabolic activity and proliferation from day 1 of the experiment. Three different concentrations of platelets were tested. It has been shown that in the first half of the experiment, the most potent concentration in regard to fibroblast proliferation and metabolic activity was the lowest concentration of platelets (sample C3). However, the differences among the platelet-functionalized samples were leveled by the end of the experiment.

We have shown bioactive substances released from platelets stimulate both fibroblasts and keratinocytes. Interactions between keratinocytes and fibroblasts gradually shift the wound healing process from inflammation to the synthesis of granulation tissue.[29] Both cell types are essential to reduce the wound volume and for proper wound closure. Currently, there are very few drugs stimulating both cell types simultaneously and the development of such a system for deep wound healing would be very beneficial.[30]

Melanocytes are cells responsible for pigmentation of the skin. The most common depigmentation disorder of the skin is vitiligo, characterized by white macules due to the loss of functional melanocytes.[31] Recently, the concept of a cellular patch has been proposed for vitiligo treatment.[25] It consists of a suitable biomaterial allowing in vitro expansion of healthy cells and providing them with mechanical support during transplantation to the site of lesion. As such material, several polymers in the form of films have been studied (polylactic acid,[32] polyvinyl chloride and silicone[33] or chitosan coated polystyrene[25]). Some of the materials have been used in clinical practice, for example polylactic acid[34] or human amniotic membrane.[35] To date, the unique properties of nanofibers have not been exploited in this application and to the best of our knowledge melanocytes cultured on nanofibrous substrates have not been described. We have shown PCL nanofibers are suitable biomaterial for melanocyte culture. Furthermore, the functionalization of nanofibers with platelets led to a significant increase in

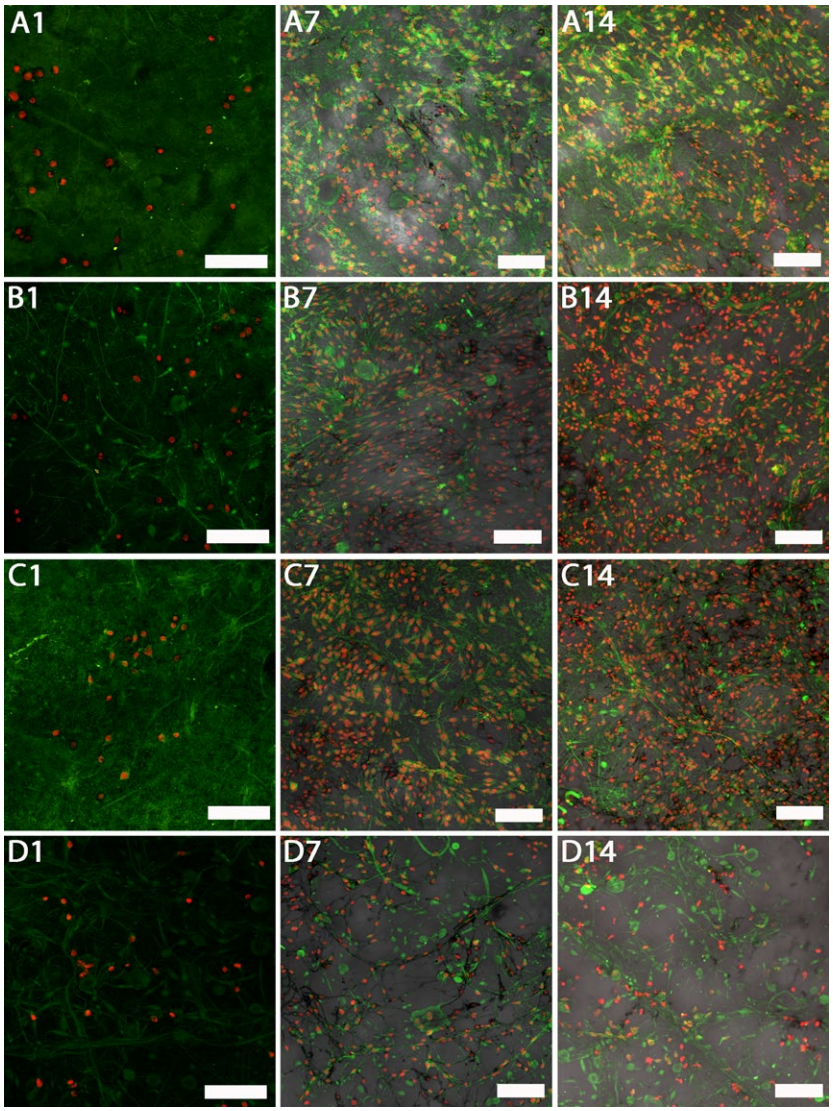

FIGURE 7 Confocal images of melanocytes cultured on platelet-functionalized PCL and PCL control scaffolds. Cellular membranes were stained by DiOC-6 (green color), cell nuclei using propidium iodide (red color). A1 – Melanocytes cultured on C1 scaffold on day 1, A7 – melanocytes cultured on C1 scaffold on day 7, A14 – melanocytes cultured on C1 scaffold on day 14, B1 – melanocytes cultured on C2 scaffold on day 1, B7 – melanocytes cultured on C2 scaffold on day 7, B14 – melanocytes cultured on C2 scaffold on day 14, C1 – melanocytes cultured on C3 scaffold on day 1, C7 – melanocytes cultured on C3 scaffold on day 7, C14 – melanocytes cultured on C3 scaffold on day 14, D1 – melanocytes cultured on PCL scaffold on day 1, D7 – melanocytes cultured on PCL scaffold on day 7, D14 – melanocytes cultured on PCL scaffold on day 14. A1, B1, C1, D1 – scale bar 100 µm, magnification 200×, A7, A14, B7, B14, C7, C14, D7, D14 – scale bar 100 µm, magnification 150×.

cell proliferation, metabolic activity and melanin synthesis. According to the confocal microscopy images, the colonization of the scaffolds by melanocytes was extremely effective. The effectiveness of the scaffold colonization is not supported by the proliferation assay data, where there is no such dramatic increase in melanocyte numbers on the platelet-functionalized samples. Such discrepancy may be caused by absorption of the PicoGreen® excitation wavelength (485 nm) by melanin, which is present in the cell lysate used for DNA quantification.

Results of the study showed that the system is able to stimulate fibroblasts, keratinocytes and melanocytes and could serve as a viable system for tissue engineering. It combines the mechanical stability of PCL nanofibers with the bioactive action of platelets. Skin repair, mainly in case of third-degree burns and diabetic ulcers, remains an important research area. Our proposed system could serve as a cell-free scaffold that promotes fibroblast and keratinocyte proliferation, migration[36] and angiogenesis via VEGF released from the adhered platelets.[23] The stimulation of keratinocyte and fibroblast growth on scaffolds should foster the healing process and may decrease the healing times as a crucial complication in chronic wounds. Additionally, after seeding with melanocytes prior to transplantation, the system could serve as a viable scaffold for vitiligo treatment. The melanocytes show good viability on scaffolds and the planar nature of platelet-functionalized scaffolds enables melanocyte application to scaffolds prior to application by spraying (i.e. ReCELL technology[37]).

No significant differences between the platelet concentrations were found, thus even the lowest tested concentration was able to stimulate the skin cells. In addition, the simple adhesion method enables fast and convenient on site preparation and rapid transfer to clinical practice. PCL is an FDA approved, biocompatible polymeric material.[38] PCL is a biodegradable polymer. Its degradation time (around 1 year) limits its use as a skin engineering product in cases when frequent change of the dressing is needed. However, PCL has been described to be susceptible to enzymatic breakdown and as the chronic wounds are characterized by excessive proteolytic activity, such phenomenon could play a part in the degradation of the polymer from the healing wound.[39]

Carter et al.[40] and their meta-analysis on available data concerning the use of platelet rich plasma in clinical practice showed PRP

therapy not only has a positive impact on the wound healing process, but is associated with reduction in pain, infection and other adverse effects of chronic wound healing as well. Our system combines both approaches and thus should facilitate healing more effectively.

ACKNOWLEDGEMENTS

This study was supported by the Grant Agency of Charles University (Grants Nos. 270513, 424213, 1246314, 1262414, 1228214, 545313), the Czech Science Foundation Grant No. 15- 15697S, the University Centre for Energy Efficient Buildings, the Ministry of Education, Youth, and Sports of the Czech Republic (Research Programs NPU I:LO1508 and NPU I:LO1309) and the Internal Grant Agency of the Ministry of Health of the Czech Republic (grant No. NT12156 and MZ-VES project no. 15-33094A).

REFERENCES

1. Crovetti G, Martinelli G, Issi M, et al. Platelet gel for healing cutaneous chronic wounds. *Transfus Apheres Sci*. 2004;30:145–151.
2. Barrientos S, Stojadinovic O, Golinko MS, Brem H, Tomic-Canic M. Growth factors and cytokines in wound healing. *Wound Repair Regen*. 2008;16:585–601.
3. Werner S, Grose R. Regulation of wound healing by growth factors and cytokines. *Physiol Rev*. 2003;83:835–870.
4. Rieger KA, Birch NP, Schiffman JD. Designing electrospun nanofiber mats to promote wound healing – a review. *J Mater Chem B*. 2013;1:4531–4541.
5. Mustoe T. Understanding chronic wounds: a unifying hypothesis on their pathogenesis and implications for therapy. *Am J Surg*. 2004;187:S65–S70.
6. Hess CT. *Wound Care*. Philadelphia: Lippincott Williams & Wilkins; 2005.
7. Zahedi P, Rezaeian I, Ranaei-Siadat SO, Jafari SH, Supaphol P. A review on wound dressings with an emphasis on electrospun nanofibrous polymeric bandages. *Polym Adv Technol*. 2010;21:77–95.
8. Chakraborty S, Liao IC, Adler A, Leong KW. Electrohydrodynamics: A facile technique to fabricate drug delivery systems. *Adv Drug Deliv Rev*. 2009;61:1043–1054.
9. Chew SY, Wen Y, Dzenis Y, Leong KW. The role of electrospinning in the emerging field of nanomedicine. *Curr Pharm Des*. 2006;12:4751–4770.
10. Chen FM, Zhang M, Wu ZF. Toward delivery of multiple growth factors in tissue engineering. *Biomaterials*. 2010;31:6279–6308.
11. Alsousou J, Thompson M, Hulley P, Noble A, Willett K. The biology of platelet-rich plasma and its application in trauma and orthopaedic surgery: a review of the literature. *J Bone Joint Surg Br*. 2009;91:987–996.
12. Foster TE, Puskas BL, Mandelbaum BR, Gerhardt MB, Rodeo SA. Platelet-rich plasma from basic science to clinical applications. *Am J Sports Med*. 2009;37:2259–2272.
13. Bennett DC, Cooper PJ, Hart IR. A line of non-tumorigenic mouse melanocytes, syngeneic with the B16 melanoma and requiring a tumour promoter for growth. *Int J Cancer*. 1987;39:414–418.
14. Busca R, Bertolotto C, Ortonne JP, Ballotti R. Inhibition of the phosphatidylinositol 3-kinase/p70(S6)-kinase pathway induces B16 melanoma cell differentiation. *J Biol Chem*. 1996;271:31824–31830.
15. Moore WS. *Vascular and Endovascular Surgery: A Comprehensive Review*. Philadelphia: Elsevier/Saunders; 2013.
16. Boswell SG, Cole BJ, Sundman EA, Karas V, Fortier LA. Platelet-rich plasma: a milieu of bioactive factors. *Arthroscopy*. 2012;28:429–439.
17. Eppley BL, Woodell JE, Higgins J. Platelet quantification and growth factor analysis form platelet-rich plasma: implications for wound healing. *Plast Reconstr Surg*. 2004;114:1502–1508.
18. Giehl KA, Nägele U, Volkenandt M, Berking C. Protein expression of melanocyte growth factors (bFGF, CSF) and their receptors (FGFR-1, c-kit) in nevi and melanoma. *J Cutan Pathol*. 2007;34:7–14.
19. Plencner M, Prosecká E, Rampichová M, et al. Significant improvement of biocompatibility of polypropylene mesh for incisional hernia repair by using poly-ε-caprolactone nanofibers functionalized with thrombocyte-rich solution. *Int J Nanomed*. 2015;10:2635.
20. Knotek P, Pouzar M, Buzgo M, et al. Cryogenic grinding of electrospun poly-ε-caprolactone mesh submerged in liquid media. *Mater Sci Eng C Mater Biol Appl*. 2012;32:1366–1374.
21. Tian F, Hosseinkhani H, Hosseinkhani M, et al. Quantitative analysis of cell adhesion on aligned micro-and nanofibers. *J Biomed Mater Res, Part A*. 2008;84:291–299.
22. Wan LS, Xu ZK. Polymer surfaces structured with random or aligned electrospun nanofibers to promote the adhesion of blood platelets. *J Biomed Mater Res, Part A*. 2009;89:168–175.
23. Laurens N, Koolwijk P, De Maat MPM. Fibrin structure and wound healing. *J Thromb Haemost*. 2006;4:932–939.
24. Kiran S, Nune KC, Misra RDK. The significance of grafting collagen on polycaprolactone composite scaffolds: processing-structure-functional property relationship. *J Biomed Res Part A*. 2015;103A:2919–2931.
25. Lin S-J, Jee S-H, Hsaio W-C, Lee S-J, Young T-H. Formation of melanocyte spheroids on the chitosan-coated surface. *Biomaterials*. 2005;26:1413–1422.
26. Jakubova R, Mickova A, Buzgo M, et al. Immobilization of thrombocytes on PCL nanofibres enhances chondrocyte proliferation in vitro. *Cell Prolif*. 2011;44:183–191.
27. Choi JS, Leong KW, Yoo HS. In vivo wound healing of diabetic ulcers using electrospun nanofibers immobilized with human epidermal growth factor (EGF). *Biomaterials*. 2008;29:587–596.
28. Liu Y, Kalén A, Risto O, Wahlström O. Fibroblast proliferation due to exposure to a platelet concentrate in vitro is pH dependent. *Wound Repair Regen*. 2002;10:336–340.
29. Werner S, Krieg T, Smola H. Keratinocyte–fibroblast interactions in wound healing. *J Investig Dermatol*. 2007;127:998–1008.
30. Shrivastava R. Clinical evidence to demonstrate that simultaneous growth of epithelial and fibroblast cells is essential for deep wound healing. *Diabetes Res Clin Pract*. 2011;92:92–99.
31. Alikhan A, Felsten LM, Daly M, Petronic-Rosic V. Vitiligo: a comprehensive overview Part I. Introduction, epidemiology, quality of life, diagnosis, differential diagnosis, associations, histopathology, etiology, and work-up. *J Am Acad Dermatol*. 2011;65:473–491.
32. Ghosh D, Shenoy S, Kuchroo P. Cultured melanocytes: from skin biopsy to transplantation. *Cell Transplant*. 2008;17:351–360.
33. Eves PC, Bullett NA, Haddow D, et al. Simplifying the delivery of melanocytes and keratinocytes for the treatment of vitiligo using a chemically defined carrier dressing. *J Investig Dermatol*. 2008;128:1554–1564.
34. Ghosh D, Kuchroo P, Viswanathan C, et al. Efficacy and safety of autologous cultured melanocytes delivered on poly (dl-lactic acid) film: a prospective, open-label, randomized, multicenter study. *Dermatol Surg*. 2012;38:1981–1990.
35. Redondo P, Giménez de Azcarate A, Marqués L, García-Guzman M, Andreu E, Prósper F. Amniotic membrane as a scaffold for melanocyte transplantation in patients with stable vitiligo. *Dermatol Res Pract*. 2011;2011:1–6.

36. Mansbridge J. Skin tissue engineering. *Journal of Biomaterials Science*, Polymer Edition. 2008;19(8):955–968.
37. Gravante G, Di Fede MC, Araco A, et al. A randomized trial comparing ReCell® system of epidermal cells delivery versus classic skin grafts for the treatment of deep partial thickness burns. *Burns*. 2007;33:966–972.
38. Cipitria A, Skelton A, Dargaville TR, Dalton PD, Hutmacher DW. Design, fabrication and characterization of PCL electrospun scaffolds-a review. *J Mater Chem*. 2011;21:9419–9453.
39. Dai NT, Williamson MR, Khammo N, Adams EF, Coombes AGA. Composite cell support membranes based on collagen and polycaprolactone for tissue engineering of skin. *Biomaterials*. 2004;25:4263–4271.
40. Carter MJ, Fylling CP, Parnell LK. Use of platelet rich plasma gel on wound healing: a systematic review and meta-analysis. *Eplasty*. 2011;11:e38.